Constructing an Average Geometry and Diffusion Tensor Magnetic Resonance Field from Freshly Explanted Porcine Hearts

Mia Mojica[a], Mihaela Pop[b], Maxime Sermesant[c], and Mehran Ebrahimi[a]

[a]Faculty of Science, University of Ontario Institute of Technology, Oshawa, ON, Canada
[b]Department of Medical Biophysics, University of Toronto, Toronto, ON, Canada
[c]Asclepios Team, INRIA Sophia Antipolis, France

ABSTRACT

The local arrangement of cardiac fibers provides insight into the electrical and mechanical functions of the heart. Fiber directions can be obtained using diffusion tensor (DT) MR imaging and further integrated into computational heart models for accurate predictions of activation times and contraction. However, this information is not available due to limitations of cardiac *in-vivo* DTI; thus, an average atlas could be used instead of individual fiber directions. In this work, we present a simple and computationally efficient pipeline for constructing a novel statistical cardiac atlas from *ex-vivo* high resolution DT images of porcine hearts. Our framework involves normalizing the cardiac geometries, reorienting local directional information on diffusion, and computing the average diffusion tensor field. The registration step eliminates the need for landmarks, while the tensor reorientation strategy enables the transformation of the diffusion tensors and preserves the diffusion tensor orientations.

Keywords: cardiac atlas, MRI, diffusion tensor imaging, elastic registration, tensor transformation

1. INTRODUCTION

Cardiovascular disease (CVD) is the leading cause of mortality, accounting annually for 17 million deaths, or around 30% of all deaths worldwide.[1] Image-based models and statistical atlases of the cardiac anatomy and physiology can aid in better diagnosis and treatment-planning of CVD.

The cardiac muscle structure is characterized by a high degree of anisotropy. The organization of parallel myofibers into bundles helps coordinate the propagation of action potential electrical wave, leading to a synchronous depolarization and contraction of left and right ventricles.[2–6] Thus, a remodeling of fiber orientations profoundly impacts the conduction properties of the heart, which is often impaired in CVD.

Fiber directions in healthy state can be determined via DT MRI and then integrated into predictive image-based heart models[7,8] and statistical atlases.[9,10] However, such information is difficult to obtain *in-vivo* due to lengthy MR imaging times. Thus, an average atlas could be used instead of individual fiber directions.

A statistical atlas of the human cardiac fiber architecture was first built by Lombaert *et al.* [11]. Their dataset consisted of 10 *ex-vivo* healthy hearts. In their study, they calculated the fiber orientation dispersion across the population. They also compared their results against previous studies on mammals and found that they yielded concurring conclusions. Peyrat *et al.* [12] presented a detailed computational framework for building a statistical atlas and applied said framework on a dataset of 9 *ex-vivo* canine hearts. They also extracted diffusion tensor statistics characterizing cardiac fiber and laminar sheet orientations. In addition, they found better stability in the statistical comparison of fiber orientations than the laminar sheet orientations between the computed canine atlas and a standard human cardiac DT-MRI.

Further author information: (Send correspondence to)
Mia Mojica: E-mail: Mia.Mojica@uoit.ca
Mihaela Pop: E-mail: Mihaela.Pop@utoronto.ca
Maxime Sermesant: E-mail: Maxime.Sermesant@inria.fr
Mehran Ebrahimi: E-mail: Mehran.Ebrahimi@uoit.ca

The goal of this work is to lay the foundation for constructing a myocardial statistical atlas from *ex-vivo* DT images of porcine hearts (with size comparable to human hearts) by computing an average geometry that models a healthy porcine heart, reorienting the tensors and projecting them onto a common reference frame, and extracting the average diffusion tensor field.

2. METHODS

The cardiac atlas construction pipeline is shown in Figure 1. Diffusion tensor images were first acquired to get directional information of diffusion. Briefly, to calculate a mean volume, the unweighted anatomical images of each subject were normalized via groupwise registration. Using the transformations from the registration step, all the original diffusion tensors were reoriented to lie in the same frame of reference. These transformed tensors were then averaged and the resulting average DT field was visualized.

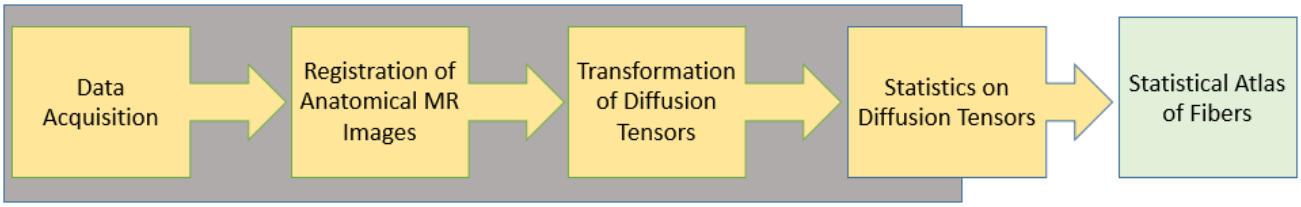

Figure 1: Workflow diagram for building a statistical porcine cardiac atlas. Diffusion-weighted MR images were acquired, and then an average cardiac geometry was constructed through groupwise registration. The final transformations for each heart were then used to project the tensors onto a common reference frame, and the average DT field was computed from these transformed tensors.

2.1 Data

All high resolution DT MR images were acquired on a 1.5T GE Signa Excite scanner in freshly explanted healthy pig hearts ($N = 6$) at sub-millimetric spatial resolution ($0.5 \times 0.5 \times 1.6$ mm). The hearts were fixed in 10% formalin for approximately 3-4 days and imaged with a diffusion-weighted sequence based on a fast spin echo (FSE) sequence.[13] We employed the following MR parameters: TE = 35 ms, TR = 700 ms, echo train length = 2, b-value = 0 for the unweighted MR images and $b = 500$ s/mm^2 for the seven diffusion gradients, respectively.[14] Notably, the total MR imaging time was approximately 10 hours/heart, which is not feasible for *in-vivo* patient studies.

For DT data processing, we employed the basic equations from fundamental theory of diffusion-weighted imaging introduced in [15]. At every voxel, the magnitude of the MR signal in a so-called spin-echo image is given by

$$S = P\left(1 - e^{-TR/T_1}\right) e^{-TE/T_2} e^{-bd},$$

where P refers to proton density, TR and TE are the repetition and echo times respectively, T_1 and T_2 are the signal relaxation times after excitation, b is the diffusion-weighting factor, and d refers to the diffusion coefficient. S is the information we obtain from MR scanners and can be interpreted as the magnitude of signal from water.[15] TR, TE, T_1, and T_2 are all measured in milliseconds (ms), b is measured in s/mm^2, and d in mm^2/s.

Two separate experiments are performed to compute the diffusion coefficient at every voxel. If we keep all the parameters fixed and only vary the diffusion-weighting factors for the two experiments, we get

$$d = -\ln\left(\frac{S_2}{S_1}\right)(b_2 - b_1),$$

with $b_1 = 0$ and $b_2 = 500$ s/mm^2 being the diffusion-weighting factors used in our experiments.

The diffusion coefficient represents the translational motion of water molecules, which is random thermal motion.[16] It is computed at every voxel for each sensitization direction applied to the MR image. In practice, at

least 6 different encoding gradients are applied to cover the 3D space in order to accurately measure the amount of diffusion at every voxel.[17,18]

For a diffusion-weighted image, diffusion at every voxel may be represented by a diffusion tensor D, which is a 3×3 symmetric positive definite matrix

$$D = \begin{bmatrix} d_{xx} & d_{xy} & d_{xz} \\ d_{xy} & d_{yy} & d_{yz} \\ d_{xz} & d_{yz} & d_{zz} \end{bmatrix}.$$

The diagonal entries d_{xx}, d_{yy}, and d_{zz} represent diffusion coefficients measured along each of the principal (x-, y-, and z-) axes, while the six off-diagonal entries reflect the correlation of random motions between each pair of principal directions. These tensors contain local information on the type, orientation and magnitude of diffusion. For instance, the eigenvector corresponding to the most dominant eigenvalue of the diffusion tensor is locally aligned with the fiber direction.[12,19,20]

2.2 Average cardiac geometry

A mean cardiac volume was generated by normalizing the anatomical structures of the subjects. This was done through an iterative groupwise registration scheme that converges to a stable average cardiac geometry.

Every groupwise step was initialized by registering each subject $\mathcal{T}_i$ $(i = 1, \ldots, N)$ to a current reference volume $\mathcal{R}^n$. This is equivalent to the following problem for the optimal transformation y^* aligning $\mathcal{T}_i$ to $\mathcal{R}^n$:

$$y^* = \min_y \mathcal{J}[y] = \mathcal{D}[\mathcal{T}_i[y], \mathcal{R}^n] + \mathcal{S}[y], \tag{1}$$

where $\mathcal{T}_i[y]$ is a transformed version of the subject.

The similarity measure used in our experiments was the Sum of Squared Distances (SSD):

$$\mathcal{D}[\mathcal{T}_i[y], \mathcal{R}^n] = \frac{1}{2} \int_\Omega \left(\mathcal{T}_i[y](x) - \mathcal{R}(x)\right)^2 \, dx. \tag{2}$$

In addition, elastic regularization was imposed to allow for dilations, translations, and rotations without shearing. It is given by

$$\mathcal{S}[y] = \frac{1}{2} \int_\Omega \mu \langle \nabla y, \nabla y \rangle + (\lambda + \mu)(\nabla \cdot y)^2 dx.$$

The following update scheme was implemented to compute a new reference volume at the end of the pairwise registration step:

$$\mathcal{R}^{n+1}_{\text{mean}}(\mathrm{x}^h) = \frac{1}{N} \sum_{i=1}^{N} \mathcal{T}_i \left(y_i^n \circ [y^n_{\text{mean}}]^{-1} (\mathrm{x}^h) \right), \tag{3}$$

where

- N refers to the size of the dataset,
- $\mathcal{T}_i$ are subjects $(i = 1, 2, \ldots N)$,
- y_i^n is the transformation aligning the i^{th} subject to the current reference.
- y^n_{mean} is the mean of the transformations y_i^n, and
- $y_i^n \circ [y^n_{\text{mean}}]^{-1}$ is the composition of y_i^n with the inverse of y^n_{mean}.

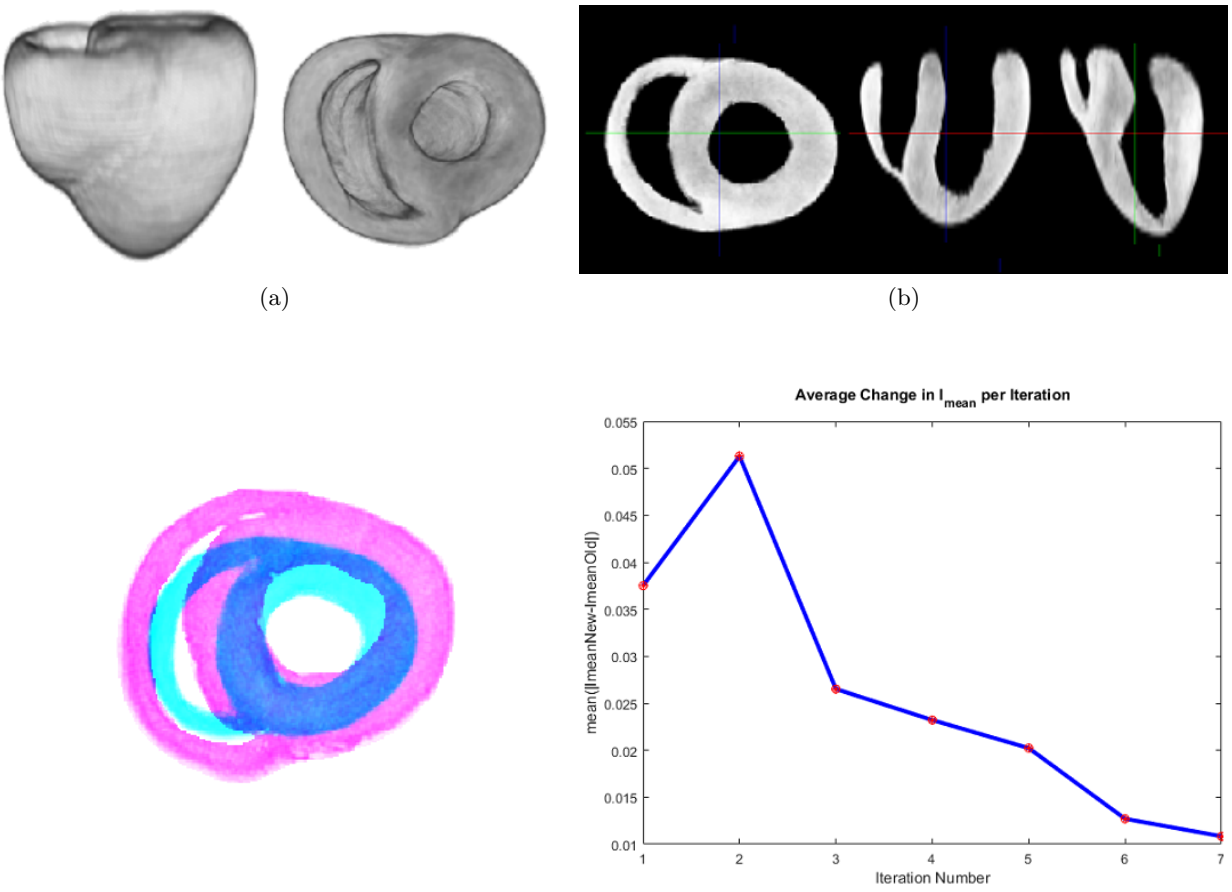

(a) (b) (c) (d)

Figure 2: Results of the groupwise registration scheme. (a) 3D and (b) cross-sectional views of the average geometry computed from 6 healthy porcine hearts, (c) evolution of the reference geometries (the first reference image overlaid onto the final average), and (d) convergence of the groupwise framework measured in terms of the average change in intensity values between successive reference geometries. Note that the values dropped by approximately 82% after the 7th iteration.

We implemented this sequence of updates until there was no more significant change between consecutive reference geometries in terms of the average change in intensity values. The method effectively normalized the cardiac geometries and converged to a stable average geometry after 7 iterations despite a high variability in terms of the size of the heart volumes. We present in Figure 2 several results of the method: the final average geometry, the evolution of the reference geometries, and the convergence of the groupwise framework measured in terms of the change in intensity values between successive reference geometries.

Due to its flexibility and array of resources for 3D to 3D registration, Jan Modersitzki's Flexible Algorithms for Image Registration (FAIR) [21] toolkit built for MATLAB* was used to solve the discretized version of the optimization problem in (1) for each pairwise alignment of cardiac volumes. We also implemented the groupwise registration framework on MATLAB for simplicity. These were all implemented on a workstation with Intel(R) Xeon(R) CPU E5-1620 v2 @ 3.70GHz with 16GB of RAM.

*®2018 The MathWorks, Inc. MATLAB and Simulink are registered trademarks of The MathWorks, Inc. See mathworks.com/trademarks for a list of additional trademarks.

2.3 Finite Strain tensor reorientation

Once the average geometry is known, the diffusion tensors then needed to be reoriented according to the modification of the reference frame[12] while retaining the underlying cardiac fiber structure. To this end, we used the Finite Strain method. The final transformations that map the hearts to the average geometry were used to transform each DT field. More specifically, the deformation gradient of the transformations were decomposed via polar decomposition and expressed as a product of a rotation and a stretch component. The reoriented tensor is then given by

$$D_i' = R \cdot D_i \cdot R^T.$$

Shown in Figure 3 are the tensors of one of the subjects reoriented via the Finite Strain method. Observe that the geometric features of the diffusion tensor field were preserved. This makes Finite Strain an ideal method for inter-subject DT-MRI registration.[12]

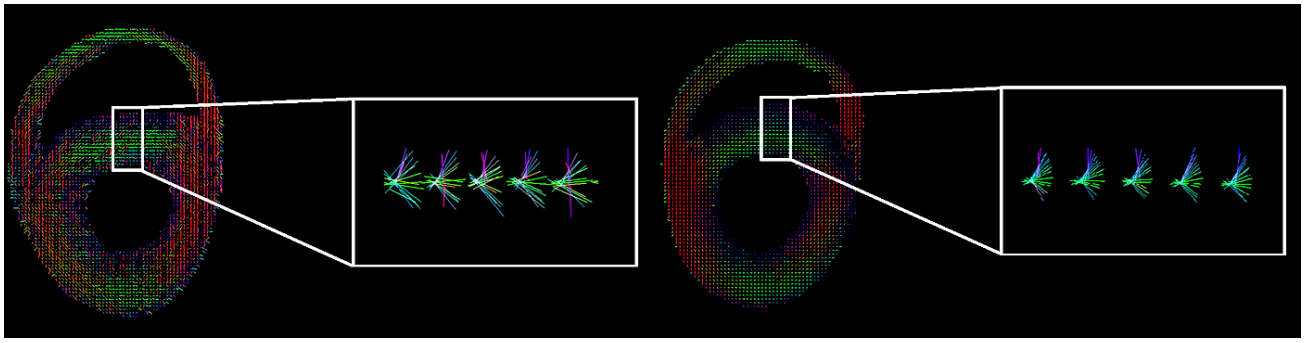

(a) (b)

Figure 3: Finite strain reorientation method. (a) Original and (b) transformed tensors of one of the subjects in the dataset generated using MedInria (http://med.inria.fr). The magnified section shows tensors viewed transmurally from an area in the septum. Observe that the geometric features of the diffusion tensor fields were preserved.

2.4 Average DT field and fiber architecture

Lastly, we calculated and visualized the mean of the transformed diffusion tensors. Note that diffusion tensors are positive-definite matrices that do not form a vector space. As a consequence, we cannot compute their Euclidean mean. To get around this, we employed Log-Euclidean metrics. These were shown to circumvent the defects of the classical Euclidean framework and, more importantly, preserve the positive-definiteness of the tensors.[22]

For every voxel X in the average geometry, the mean $\overline{D}_{\log}$ of the transformed diffusion tensors D_i' is

$$\overline{D}_{\log}(X) = \exp\left(\frac{1}{N}\sum_{i=1}^{N}\log\left(D_i'\left(X\right)\right)\right).$$

MedInria [23] was used to visualize the average DT field (shown in Figure 4).

3. CONCLUSIONS

In our work, we laid the groundwork for building a statistical cardiac atlas from six explanted healthy porcine hearts. More importantly, we have created the first atlas for porcine hearts by proposing a simple multilevel elastic registration approach to match pairs of cardiac volumes without the need for landmarks, computed a representative (average) geometry and the associated diffusion tensor field, which contains local diffusion information. Future work will be focused on adding more data, mapping out the average fiber architecture, and extracting tensor statistics for the fiber atlas.

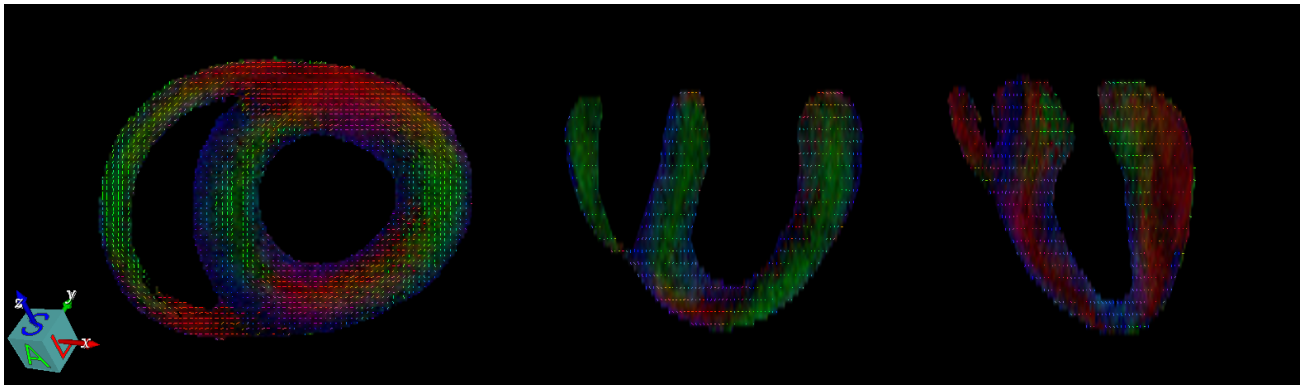

Figure 4: Average DT field. Different cross-sectional views of the average tensor field visualized through MedInria. The tensors are red when the primary eigenvector is oriented along the direction of the x-coordinates, green along the direction of the y-coordinates, and blue along the direction of the z-coordinates.

The work presented here is novel and represents a logical next step for our previous work [24], which was solely focused on computing an average geometry from a small database of four porcine hearts. It was published at a MICCAI workshop: International Workshop on Statistical Atlases and Computational Modeling of the Heart (STACOM) 2017. Since then, we have added more healthy hearts in our experiments and updated all our previously published results.

ACKNOWLEDGMENTS

This work was supported in part by an NSERC Discovery grant and Deborah Saucier Early Researcher Award for Dr. Mehran Ebrahimi, and an Inria - Associated team grant for Drs. Mihaela Pop and Maxime Sermesant. Mia Mojica is supported by an Ontario Trillium Scholarship (OTS).

REFERENCES

[1] World Health Organization, "Cardiovascular Diseases." http://www.who.int/mediacentre/factsheets/fs317/en (2017). [Online; accessed 20-January-2019].

[2] Peyrat, J.-M., *Comparison of cardiac anatomy and function: statistics on fibre architecture from DT-MRI and registration of 4D CT Images*, PhD thesis, Université Nice Sophia Antipolis (2009).

[3] Helm, P. A., "A novel technique for quantifying variability of cardiac anatomy: Application to the dyssynchronous failing heart.," (2004).

[4] Beg, M. F., Helm, P. A., McVeigh, E., Miller, M. I., and Winslow, R. L., "Computational cardiac anatomy using mri," *Magnetic resonance in medicine* **52**(5), 1167–1174 (2004).

[5] Caldwell, B. J., Trew, M. L., Sands, G. B., Hooks, D. A., LeGrice, I. J., and Smaill, B. H., "Three distinct directions of intramural activation reveal non–uniform side–to–side electrical coupling of ventricular myocytes," *Circulation: Arrhythmia and Electrophysiology* , CIRCEP–108 (2009).

[6] Piuze-Phaneuf, E., *The Geometry of Cardiac Myofibers*, PhD thesis, McGill University Libraries (2015).

[7] Pop, M., Sermesant, M., Lepiller, D., Truong, M. V., McVeigh, E. R., Crystal, E., Dick, A., Delingette, H., Ayache, N., and Wright, G. A., "Fusion of optical imaging and mri for the evaluation and adjustment of macroscopic models of cardiac electrophysiology: a feasibility study," *Medical image analysis* **13**(2), 370–380 (2009).

[8] Pop, M., Sermesant, M., Mansi, T., Crystal, E., Ghate, S., Peyrat, J.-M., Lashevsky, I., Qiang, B., McVeigh, E., Ayache, N., et al., "Correspondence between simple 3-d mri-based computer models and in-vivo ep measurements in swine with chronic infarctions," *IEEE Transactions on Biomedical Engineering* **58**(12), 3483 (2011).

[9] Toussaint, N., Sermesant, M., Stoeck, C. T., Kozerke, S., and Batchelor, P. G., "In vivo human 3d cardiac fibre architecture: reconstruction using curvilinear interpolation of diffusion tensor images," in [*International Conference on Medical Image Computing and Computer-Assisted Intervention*], 418–425, Springer (2010).

[10] Toussaint, N., Stoeck, C. T., Schaeffter, T., Kozerke, S., Sermesant, M., and Batchelor, P. G., "In vivo human cardiac fibre architecture estimation using shape-based diffusion tensor processing," *Medical image analysis* **17**(8), 1243–1255 (2013).

[11] Lombaert, H., Peyrat, J.-M., Croisille, P., Rapacchi, S., Fanton, L., Cheriet, F., Clarysse, P., Magnin, I., Delingette, H., and Ayache, N., "Human atlas of the cardiac fiber architecture: study on a healthy population," *IEEE transactions on medical imaging* **31**(7), 1436–1447 (2012).

[12] Peyrat, J.-M., Sermesant, M., Pennec, X., Delingette, H., Xu, C., McVeigh, E. R., and Ayache, N., "A computational framework for the statistical analysis of cardiac diffusion tensors: application to a small database of canine hearts," *IEEE Transactions on medical imaging* **26**(11), 1500–1514 (2007).

[13] Helm, P. A., Tseng, H.-J., Younes, L., McVeigh, E. R., and Winslow, R. L., "Ex vivo 3d diffusion tensor imaging and quantification of cardiac laminar structure," *Magnetic resonance in medicine* **54**(4), 850–859 (2005).

[14] Pop, M., Ghugre, N. R., Ramanan, V., Morikawa, L., Stanisz, G., Dick, A. J., and Wright, G. A., "Quantification of fibrosis in infarcted swine hearts by ex vivo late gadolinium-enhancement and diffusion-weighted mri methods," *Physics in Medicine & Biology* **58**(15), 5009 (2013).

[15] Mori, S. and Zhang, J., "Principles of diffusion tensor imaging and its applications to basic neuroscience research," *Neuron* **51**(5), 527–539 (2006).

[16] Huisman, T., "Diffusion-weighted and diffusion tensor imaging of the brain, made easy," *Cancer Imaging* **10**(1A), S163 (2010).

[17] Kingsley, P. B., "Introduction to diffusion tensor imaging mathematics: Part i. tensors, rotations, and eigenvectors," *Concepts in Magnetic Resonance Part A* **28**(2), 101–122 (2006).

[18] Kingsley, P. B., "Introduction to diffusion tensor imaging mathematics: Part ii. anisotropy, diffusion-weighting factors, and gradient encoding schemes," *Concepts in Magnetic Resonance Part A* **28**(2), 123–154 (2006).

[19] Scollan, D. F., Holmes, A., Winslow, R., and Forder, J., "Histological validation of myocardial microstructure obtained from diffusion tensor magnetic resonance imaging," *American Journal of Physiology-Heart and Circulatory Physiology* **275**(6), H2308–H2318 (1998).

[20] Hsu, E., Muzikant, A., Matulevicius, S., Penland, R., and Henriquez, C., "Magnetic resonance myocardial fiber-orientation mapping with direct histological correlation," *American Journal of Physiology-Heart and Circulatory Physiology* **274**(5), H1627–H1634 (1998).

[21] Modersitzki, J., [*FAIR: Flexible algorithms for image registration*], vol. 6, SIAM (2009).

[22] Arsigny, V., Fillard, P., Pennec, X., and Ayache, N., "Log-euclidean metrics for fast and simple calculus on diffusion tensors," *Magnetic Resonance in Medicine: An Official Journal of the International Society for Magnetic Resonance in Medicine* **56**(2), 411–421 (2006).

[23] Toussaint, N., Souplet, J.-C., Fillard, P., et al., "Medinria: Medical image navigation and research tool by inria," in [*Proc. of MICCAI*], **7**, 280 (2007).

[24] Mojica, M., Pop, M., Sermesant, M., and Ebrahimi, M., "Multilevel non-parametric groupwise registration in cardiac MRI: Application to explanted porcine hearts," in [*International Workshop on Statistical Atlases and Computational Models of the Heart*], 60–69, Springer (2017).